






Article

Thermal Hazard and Smoke Toxicity Assessment of Building Polymers Incorporating TGA and FTIR—Integrated Cone Calorimeter Arrangement

Preeti Moni Doley ¹, Anthony Chun Yin Yuen ^{1,*}, Imrana Kabir ¹, Luzhe Liu ¹, Cheng Wang ¹, Timothy Bo Yuan Chen ¹ and Guan Heng Yeoh ^{1,2}

¹ School of Mechanical and Manufacturing Engineering, University of New South Wales, Sydney, NSW 2052, Australia

² Australian Nuclear Science and Technology Organisation (ANSTO), PMB 1, Menai, NSW 2234, Australia

* Correspondence: c.y.yuen@unsw.edu.au; Tel.: +61-2-93855697

Abstract: Building polymers are highly flammable and produce a vast amount of toxic chemical compounds in the event of a fire which can lead to potential incapacitation and death. To gain an in-depth understanding of this issue, smoke toxicity and thermal characteristics of seven commonly used building polymers were analysed through a systematic fire performance evaluation system using a Thermogravimetric Analyzer and a Cone Calorimeter coupled with an FTIR arrangement. Four Fractional Effective Dose (FED) expressions were compared to assess the smoke toxicity of the fire effluents based on different assumptions. It was found that FED_{N_2} , calculated using Purser's equation, reported the highest values of FED with the following order of potential smoke toxicity at 50 kW/m² radiative heat flux: LDPU > HDPU > PE > HDEPS > XPS > EVA > LDEPS. Furthermore, fire performance evaluation of the polymers was carried out by considering three key fire risk parameters, i.e., flashover propensity, total heat released, and toxic hazard. At 50 kW/m² radiative heat flux, HDPU exhibited 11.7 times flashover propensity compared to the least flammable polymer (HDEPS), EVA exhibited 5 times total heat release compared to the polymer with the lowest total heat release (LDEPS) and, LDPU exhibited 6.7 potential times toxic hazard compared to the least toxic polymer (EVA).

Keywords: smoke toxicity; FED; fire behaviour; FTIR; cone calorimeter



Citation: Doley, P.M.; Yuen, A.C.Y.; Kabir, I.; Liu, L.; Wang, C.; Chen, T.B.Y.; Yeoh, G.H. Thermal Hazard and Smoke Toxicity Assessment of Building Polymers Incorporating TGA and FTIR—Integrated Cone Calorimeter Arrangement. *Fire* **2022**, *5*, 139. <https://doi.org/10.3390/fire5050139>

Academic Editors: Guan-Yuan Wu, Chao Zhang, Young-Jin Kwon and Nugroho Yulianto Sulisty

Received: 17 August 2022

Accepted: 15 September 2022

Published: 18 September 2022

Publisher's Note: MDPI stays neutral with regard to jurisdictional claims in published maps and institutional affiliations.



Copyright: © 2022 by the authors. Licensee MDPI, Basel, Switzerland. This article is an open access article distributed under the terms and conditions of the Creative Commons Attribution (CC BY) license (<https://creativecommons.org/licenses/by/4.0/>).

1. Introduction

With the increasing use of combustible external cladding, fire safety has become a priority for the building construction industry. A few fire incidents involving combustible claddings include the Television Cultural Centre Fire in China, involving extruded polystyrene (XPS) [1], the Shanghai Apartment Fire in China, involving polyurethane (PU) [2], and the Lacrosse Building Fire in Australia, involving polyethylene (PE) [3]. Another recent example is the Grenfell Tower fire in the UK involving a rainscreen façade system with polyisocyanurate foam insulation and aluminum polyethylene composite exterior [4]. Lightweight composite materials are extensively replacing traditional building materials, enhancing the aesthetics of buildings at a lower cost with increasing energy efficiency. These materials are often installed as insulation components in exterior wall assemblies, such as exterior insulation finish systems (EIFS) and weather-resistive barriers (WRB) [5]. Some of the commonly installed exterior cladding systems are sandwich panels consisting of a highly combustible polymeric core such as polystyrene (PS), polyisocyanurate (PIR), polyurethane (PU), and polyethylene (PE) with a thin outer metal skin made of aluminium or steel [6,7]. The polymeric cores present high fire risks for the claddings, with a potential to develop into an uncontrollable blaze on the external surfaces within 10–15 min as witnessed in many past cladding fires [8]. Additionally, combustible polymers

are also commonly used in houses as upholstered items, such as furniture foams and mattresses. A report by the National Fire Protection Association's (NFPA) Fire Incident Data Organization (FIDO) database suggests that in the past, furniture fires were the largest contributor to fire deaths in the US [9]. Although this number has declined over the years as a result of various interventions from the regulators, furniture fires are still one of the top contributors to fire deaths [10]. Overall, the use of polymers in residential and commercial buildings as insulation and furnishing materials raises concerns as it can undergo rapid combustion, releasing a high level of heat and toxic gases, especially in compartment fires, posing significant fire risks to building occupants, property, and the economy [11].

Lightweight building polymer composites are commonly utilized in modern high-rise constructions owing to their flexibility, ease to manufacture, thermal insulative and sound absorption properties. However, intrinsic flammability and toxicity of polymeric materials remain a critical issue in building fires [12,13]. Herein, inhalation of toxic smoke is generally recognized as one of the main causes of deaths and injuries during fire events [14]. According to Fire Safe Europe [15], more than half of the fire deaths and injuries in Europe were due to fire smoke. The toxicity of fire effluent during combustion depends on the chemical composition of the material and its burning conditions, such as thermal exposure conditions, fuel type, and ventilation. Smoke effluent during building fires has the potential to cause various toxicological effects in humans [16] as it can contain a very complex mixture of gases, solid particulates, liquid aerosols, and free radicals [17,18]. Asphyxiant effects and sensory or upper respiratory irritations are the predominant acute toxicity symptoms due to smoke inhalation. ISO 13344 [19] has identified the following gases that contribute to fire toxicity: (i) Asphyxiant gases: carbon monoxide, carbon dioxide, hydrogen cyanide, and oxygen depletion (with a small contribution from oxides of nitrogen); and (ii) Irritants: inorganic acid gases (hydrogen halides, sulphur oxides, nitrogen oxides, phosphoric acid), organic irritants, and smoke particulates. Smoke from a fire can also impair vision and obscure evacuation routes and act as a radiation transfer medium to cause other flammable materials to lit up, which may limit the capability of evacuees to escape the scene of fire [20,21]. The toxicity of fire effluent materials is commonly expressed in terms of Fractional Effective Dose (FED). ISO 13344 [22] defines FED as "the ratio of the concentration and time product for a gaseous toxicant produced in a given test to that product of that toxicant that has been statistically determined from independent experimental data to produce lethality in 50% of test animals within a specified exposure and postexposure period". Therefore, when the FED of the gaseous mixture is 1, it would be lethal to 50% of the exposed population. International standards such as ISO 13344 [19], ISO 13571 [23], ISO 9122-4 [24], ASTM E 1678-02 [25], and NFPA 269 [26] have considered various models for estimating the toxic potency of fire effluents. Nevertheless, there is a lack of homogeneity in the standards available for toxicity assessment as the test procedures, calculation methods prescribed, and the types of gas species considered are not consistent among these standards [27]. Most of the work on fire performance assessment of building materials excludes smoke toxicity as a key parameter and is mostly focused on thermal aspects like flammability and heat release rate. Furthermore, many countries across the globe are yet to include fire smoke toxicity assessment as part of their fire safety requirements for building materials [11].

Over the past decade, several literature studies have been carried out to study the thermal degradation and evolution of gas volatiles resulting from the polymer degradation process [28]. Sharma et al. [29] investigated the role of chimney-effect on the vertical fire spread in a rainscreen façade system for various combinations of exterior claddings and insulation materials (expandable polystyrene, polyisocyanurate, and mineral wool). Thermal properties of the façade materials were examined using Thermo-gravimetric Analysis. Thermal analysis of the polymers showed complete thermal decomposition with very less residual weight, indicating high combustibility. Furthermore, 3 to 6 times magnification of mass burning rate and flame spread were observed due to chimney-effects accompanied by heavy dripping and structural failure. A comprehensive review on fire

behaviours of PU foams by Singh et al. [30] reported 25 published works on combustion toxicity of rigid and flexible PU foams. These studies reported the production of a large quantity of visual obscuring smoke with a high concentration of HCN and CO during the combustion process. Chow et al. [31] compiled toxic gas data from various materials including building polymers burned under bench-scale and full-scale test conditions for smoke toxicity assessment. However, this study only considers CO, CO₂, and oxygen concentration for the smoke toxicity assessment. Stec et al. [32] carried out the toxicity assessment of six commonly used building insulation materials using ISO TS 19700 steady state tube furnace test for glass wool (GW), stone wool (SW), expanded polystyrene (EPS), phenolic foam (PhF), polyurethane (PU), and polyisocyanurate (PIR). It was reported that GW and SW failed to ignite under the test conditions while a significant release of HCN was recorded for PIR and PU contributing to their high toxicity. Another study carried out by McKenna et al. [4] conducted micro and bench-scale testing to assess the fire behaviour and toxic emissions of different façade products including those used in the Grenfell Tower. The study found PE-aluminium composite material (ACM) to exhibit 55 times peak heat release rates and 70 times total heat release compared to the least flammable panel with a possibility of rapid-fire spread in the external cladding, releasing significant toxic emissions. Two recent publications by Peck et al. [33] carried out testing in a large-scale BS 8414 test wall and BS 8414-1 façade flammability tests to compare the smoke toxicity and burning behaviour of four different types of rain-screen façade systems (ACM) with polyisocyanurate (PIR), phenolic foam (PhF), stone wool (SW) insulation, and polyethylene (PE) filled with PIR insulation fillings. The smoke toxicity study found that occupants exposed to emissions from PIR and PF are predicted to collapse within a few minutes of exposure, which will impede their ability to escape, leading to inhalation of lethal concentrations of asphyxiant gases (CO and HCN) [33]. Furthermore, in the flammability test, the façade system melted away, losing its structural integrity and contributing to rapid flame spread [34]. Guillaume et al. [35] investigated the façade fire propagation and gases evolved from nine different compositions of ACMs with several insulants using an intermediate-scale test method as per ISO 13785-1 standard. The study found that ACMs with a PE core have the highest peak heat release rates, significantly higher than different grades of reduced-combustibility Alpolc ACMs. Furthermore, ACMs with a PE core also exhibited the highest smoke production rates, with various toxic gas species like unburnt hydrocarbons, methane, ethylene, acetylene, and propane present in the smoke effluent. Overall, it was found that the use of polymers in buildings and furniture has the potential to ignite and cause rapid fire to spread, releasing a high concentration of toxic gases that can considerably impede the ability to escape during fire events or even cause deaths. In particular, the root cause of flashover in most compartment fires is due to upholstery soft furnishing polymers such as PU, PE based foams [36–38]. Therefore, to consider a full range of probable fire hazards associated with polymeric materials, there is a need to understand both thermal aspects and toxicity characteristics under various fire scenarios [27].

The current work focuses on assessing the thermal characteristics and potential smoke toxicity under well-ventilated fire scenarios for a selective range of commonly used building polymers for fire hazard assessment. Seven polymeric samples readily available in Australia, marketed as insulation and furnishing foams, were selected for the testing. The samples were analysed using a Thermogravimetric Analyser (TGA) and a Cone Calorimeter (CC) integrated with a Fourier Transform Infrared Spectroscopy (FTIR) instrument to evaluate the thermal characteristics and potential smoke toxicity under various well-ventilated burning conditions. Cone calorimeter (CC) tests have great potential to provide reasonable insight into many useful intrinsic material properties at reduced time and cost. The CC-FTIR arrangement is an improvement over the existing practices of reporting the toxic species that evolved during combustion using the Oxygen Consumption method as done in many studies [39,40]. The CC testing (Oxygen Consumption method) reports only a few asphyxiant gases for the toxicity assessment, such as oxygen, carbon dioxide, and carbon monoxide, due to the limitation of the CC equipment to capture a broader range of gas

species. Neglecting the presence of other toxic gas species can lead to an underestimation of the potential toxicity of fire effluents, specifically if fire retardants and other additives are added to the polymers [11]. This article aims to evaluate the potential fire hazard of some commonly used polymers by achieving the following objectives: (i) assess the thermal stability, ignitability, flammability, extinguishment, smoke release, and mass loss profile by interpreting the TGA and CC test data, (ii) analyse various toxic gas species released during the flaming process of the polymers by using the CC integrated FTIR data, (iii) compare the potential smoke toxicity of the fire effluents of the polymers in a well-ventilated burning condition by using four FED expressions with different assumptions, and (iv) evaluate the overall potential fire hazards of the samples by considering three fire hazard parameters, i.e., flashover propensity, total heat released, and potential smoke hazard. It should be noted that the CC test results are limited for a specific fire scenario and therefore the absolute ranking of polymers using the test results is limited. The relationship of smoke produced in bench scale testing, such as the CC testing, to that of a large-scale testing is complex and remains an open question till date. Quintiere [41] reviewed various scaling techniques such as Froude modelling, pressure modelling, and analog modelling. The review also discussed several fire problems using these strategies, such as characteristics of fire plume, burning rates of various fuels, and flame spread on materials. Despite the theoretical basis for modelling, the author acknowledges the limitations of realistic scale studies due to the complex nature of fire.

2. Materials and Methods

2.1. Sample Preparation

Seven different types of polymeric foams, HDEPS, LDEPS, EVA, LDPU, HDPU, PE and XPS (detailed in Table 1), were evaluated. The polymers were sourced from an Australian supplier, Foam Sales [42], and are marketed as readily available insulation and furnishing materials.

Table 1. Material sample abbreviations and properties.

Material	Abbr.	Density Range (kg/m ³)	Thickness (mm)
High Density Expanded Polystyrene	HDEPS	34–35	25
Low Density Expanded Polystyrene	LDEPS	20–21	25
Ethylene Vinyl Acetate	EVA	81–82	25
Low-Density Polyurethane	LDPU	33–34	25
High-Density Polyurethane	HDPU	41–42	25
Polyethylene	PE	36–39	30
Extruded Polystyrene	XPS	43–45	30

2.2. Experimentation

2.2.1. Thermo Gravimetric Analyser (TGA)

Thermogravimetric analysis was performed on a TG 209 F1 Libra[®] thermo-analyser developed by the NETZSCH Group, Germany [43], to analyse the thermal degradation of polymer samples as a function of temperature. Approximately 10 mg ± 1 mg of sample masses were thermally decomposed in an inert nitrogen atmosphere with a flow rate of 20 mL per minute with protective gas with a flow rate of 10 mL per minute, and a constant heating rate of 20 K/min over a temperature range of 20 °C to 900 °C.

2.2.2. Cone Calorimeter (CC)

A cone calorimeter (CC), the iCone[®] Classic, developed by Fire Testing Technology (FTT) Ltd., East Grinstead, UK [44], was used for testing the samples according to the standard procedure prescribed in ISO 5660-1 [45]. The test specimens were cut into 100 mm by 100 mm squares with varying thicknesses ranging from 25 to 30 mm (detailed in Table 1). The samples were tested in horizontal orientation (face up), exposed to two different heat fluxes, 35 kW/m² and 50 kW/m² using spark ignition, under standard free ventilation at ambient temperature and pressure, and a nominal exhaust extraction rate of 0.026 m³/s. The two heat fluxes selected for the test correspond to those found in developing fires. The lower heat flux, 35 kW/m², signifies a heat value that can easily induce ignition on an item in contact with another burning item [46]. The higher value, 50 kW/m², corresponds to more fully developed fires with clearer defined ignition and shorter burning time [47]. The bottom and sides of each test sample were wrapped in a single layer of aluminium foil and placed at a separation of 25 mm from the cone heater. The calibration was performed as per ISO 5660 to ensure reproducibility and precision of measurements.

The bench-scale CC test provides comprehensive data on key fire performance indicators of test samples, including flammability, ignitability, and smoke generation, in a well-ventilated fire scenario. The following important thermal parameters of the samples were deduced from the cone data (detailed in Table A1): Time to ignition (TTI) in s, peak heat release rate (pHRR) in kW/m², total heat released (THR) in MJ/m², total smoke released (TSR), a non-dimensional quantity, smoke production rate (SPR) in m²/s, and mass loss (ML) in g.

2.2.3. Fourier-Transform Infrared Spectroscopy (FTIR)

An FTIR model, atmosFIR [48] developed by Protea Ltd., UK, was coupled with the CC to continuously monitor the smoke emissions during the fire testing process. A heated sample line at 180 °C was used to transfer gas samples from the CC to the FTIR. A heated sampling line was used to prevent the condensation of species, mainly hydrocarbons, and aldehydes in the sampling system [49]. The typical measurement range of the FTIR is 0–10,000 ppm with a detection limit of <0.2 ppm. The FTIR used in this study can be configured to meet the requirements of ISO 19702 [50]. It can detect all the major gas species that are present in the fire effluent including CO, HCN, HCl, Formaldehyde, and Acrolein. The ranges of detection and lower detection limit of some of the major gas components in the smoke effluent are given in Table 2.

Table 2. Standard Analysis Model ranges for common emission species.

Component	Ranges/mg/m ³	Lower Detection Limit (LDL)/mg/m ³ , %
CO	0–1000	0.6
HCl	0–100	0.2
HF	0–50	0.2
SO ₂	0–1000	0.6
NO ₂	0–600	0.6
NO	0–600	1.0
N ₂ O	0–400	0.4
C ₃ H ₄ O	0–100	0.2
CO ₂	0–20%	0.005%

3. Results and Discussions

3.1. Thermal Degradation

The thermal stability of the samples in an inert nitrogen environment was examined by performing the TGA testing at a 20 K/min heating rate and thereby evaluating the

thermal degradation (TG) and differential thermal degradation (DTG) curves as shown in Figure 1a–g.

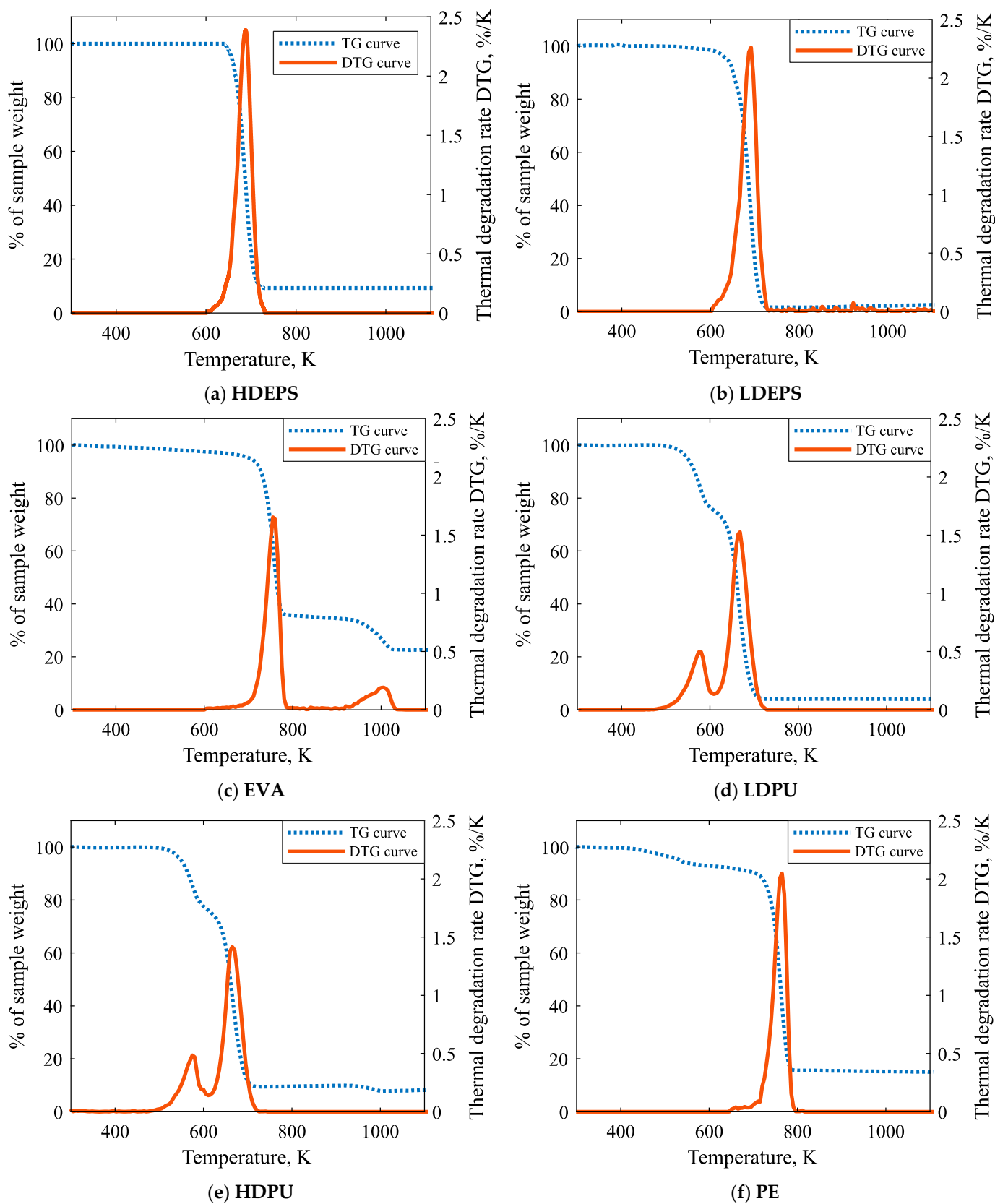


Figure 1. Cont.

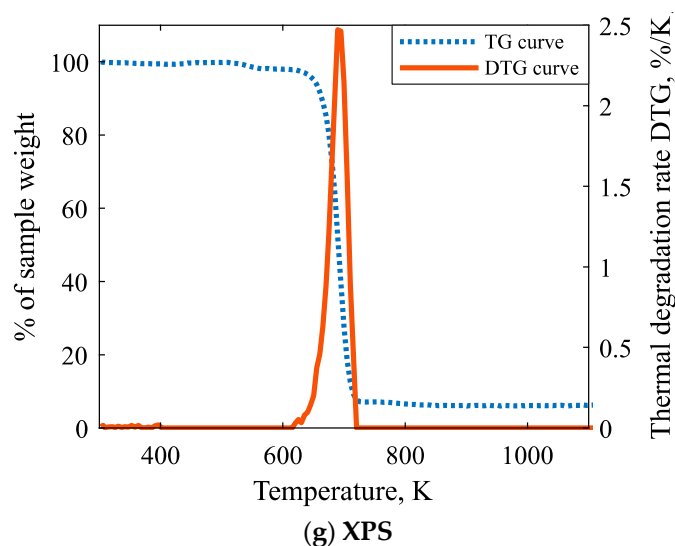


Figure 1. TG and DTG curves of polymer samples at 20 K/min heating rate: (a) HDEPS; (b) LDEPS; (c) EVA; (d) LDPU; (e) HDPU; (f) PE; (g) XPS.

The TG curve illustrates the change in mass with increasing temperature during the thermal decomposition process while the DTG curve, which is derived from the TG curve, shows the mass loss rate with increasing temperature or time. The temperatures at which the polymers undergo various stages of degradation, as well as the residual weight, are summarised in Table 3. The temperature at which the test samples lose 5% of their initial weight, denoted by $T_5\%$, signifies the onset of thermal degradation. PE underwent the earliest degradation at 520.3 K ($T_5\%$) while HDEPS exhibited the highest inertia towards initial degradation at 665.3 K ($T_5\%$). EVA, LDPU, and HDPU exhibited two stages of degradation with peak temperatures denoted by T_{max1} (major peak) and T_{max2} (minor peak), suggesting two stages of pyrolysis reactions, while PE, XPS, LDEPS, and HDEPS underwent only one stage of decomposition denoted by peak temperature T_{max1} . Both LDPU and HDPU demonstrated the least thermal stability with the lowest peak temperatures at 667.9 K (T_{max1}) and 587.9 K (T_{max2}) for LDPU and 665.1 K (T_{max1}) and 574.8 K (T_{max2}) for HDPU. It can be seen from Figure 1d,e that, for both LDPU and HDPU, approximately 22% mass loss occurred in the first stage of degradation while much of the mass loss of about 65–72% took place in the second stage of degradation. On the other hand, EVA exhibited the best thermal performance with the highest peak temperatures, 755.3 K (T_{max1}) and 1005.61 K (T_{max2}). Additionally, it can be seen from Figure 1c that, for EVA, most of the mass loss of approximately 60% took place in the first stage of degradation while a minor mass loss of approximately 17% was recorded in the second stage of degradation retaining maximum residual weight of 22.7%. The DTG curve shows that the polystyrenes exhibited the highest peaks of degradation rates of 2.46%/K for XPS, 2.36%/K for HDEPS, and 2.27%/K for LDEPS. This is due to the sudden drop in the sample mass around the peak temperature, suggesting a high rate of mass loss in a shorter span of time. Furthermore, the polystyrenes underwent complete thermal decomposition, leaving very less residue, with LDEPS and HDEPS having residual weights 2.6% and 9.8%, respectively. This finding is comparable to the literature where the TGA analysis of EPS reported a 10% residual weight indicating high combustibility [29]. The polyurethanes exhibited the lowest peaks of degradation rates with main peaks of 1.29%/K for HDPU and 1.41%/K for LDPU, and minor peaks of 0.48%/K for HDPU and 0.36%/K for LDPU. This is due to the sustained burning of the polyurethanes samples in a longer span of time around two peak temperatures. Furthermore, ethylene exhibited moderate peaks of degradation rates compared to the other samples with a major peak of 1.77%/K for PE and major and minor peaks of 1.65%/K and 0.19%/K, respectively, for EVA.

Table 3. Summarised TGA results of the test samples at 20 K/min heating rate.

Sample	Heating Rate	The Temperature at 5% Mass Loss	Main Peak Temperature	DTG (Main Peak)	Minor Peak Temperature	DTG (Minor Peak)	Residual Weight
	β (K/min)	$T_5\%$ (K)	T_{max1} (K)	%/K	T_{max2} (K)	%/K	Wt.%
HDEPS	20	665.3	699.9	2.36	-	-	9.8
LDEPS	20	663.6	702.2	2.27	-	-	2.6
EVA	20	658.4	755.3	1.65	1005.61	0.19	22.7
LDPU	20	548.1	667.9	1.41	587.905	0.36	6.1
HDFPU	20	545.2	665.1	1.29	574.8	0.48	13.1
PE	20	520.3	755.3	1.77	-	-	18.5
XPS	20	645.3	694.8	2.46	-	-	6.5

3.2. Reaction to Fire Properties

The comprehensive set of fire parameters deduced from the CC testing is discussed in this section. The deduced thermal and smoke characteristics of the polymer samples from the CC burning tests are shown in Figures 2–5.

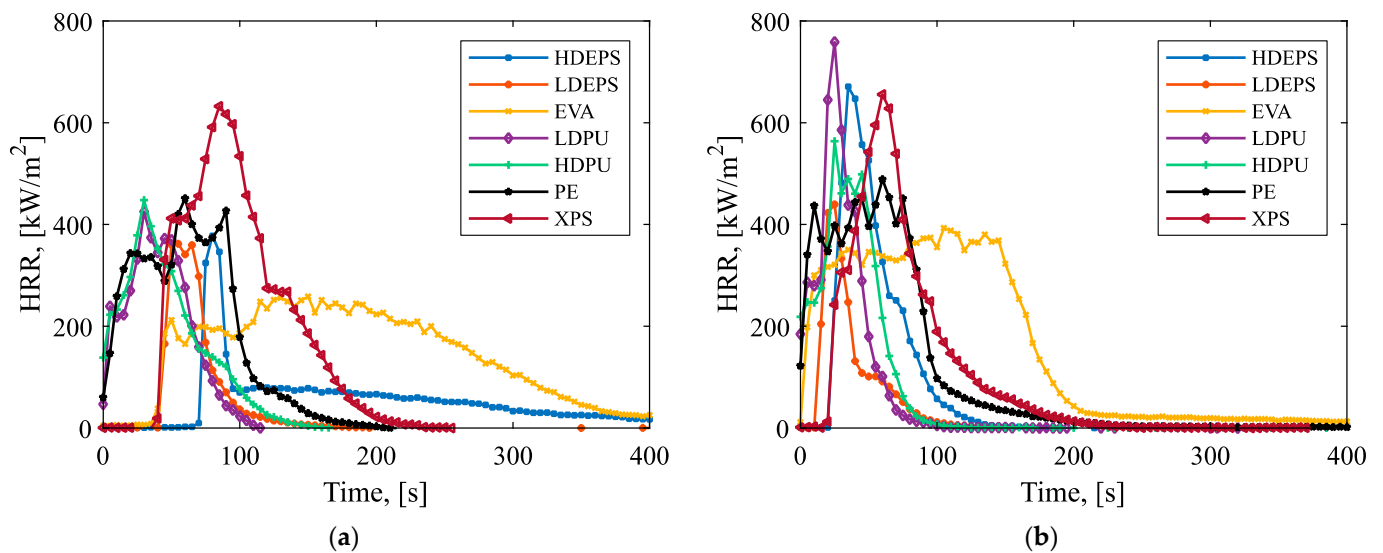


Figure 2. HRR time profile of polymer samples at (a) 35 kW/m²; (b) 50 kW/m² heat fluxes.

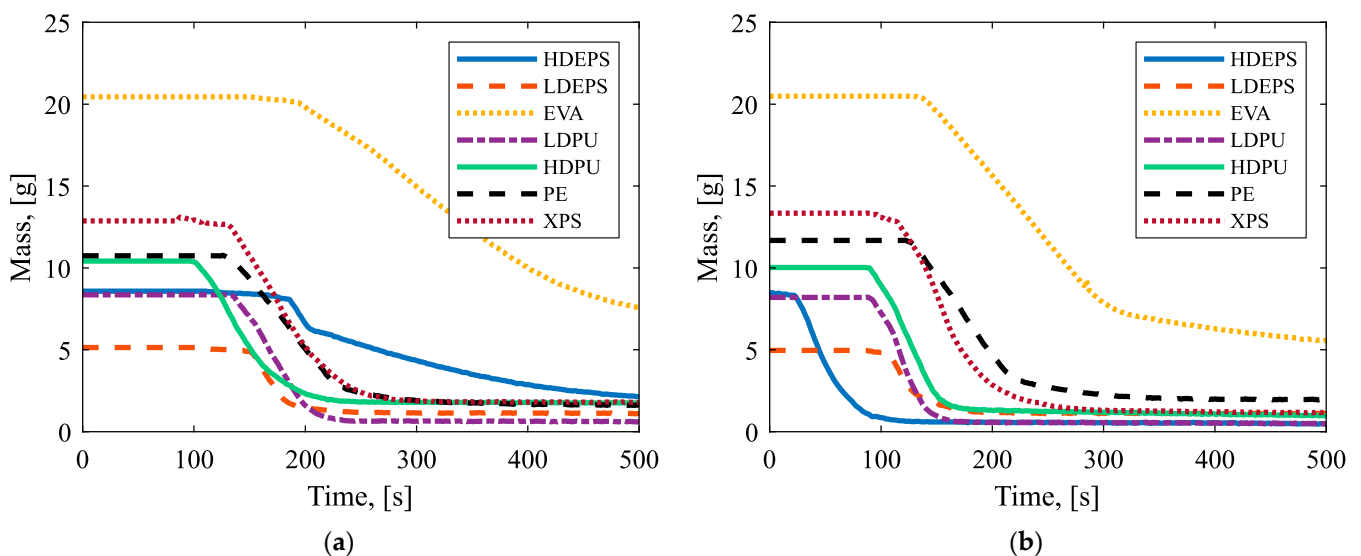


Figure 3. Mass loss time profile of polymer samples at (a) 35 kW/m²; (b) 50 kW/m² heat fluxes.

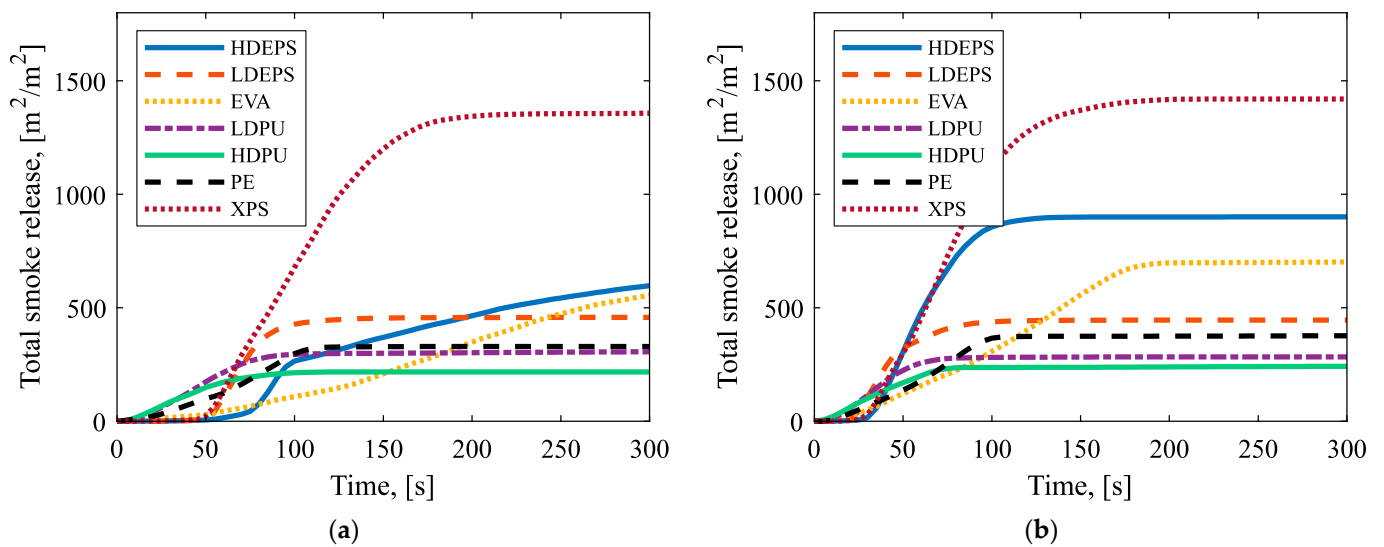


Figure 4. TSR time profile of polymer samples at (a) $35 \text{ kW}/\text{m}^2$; (b) $50 \text{ kW}/\text{m}^2$ heat fluxes.

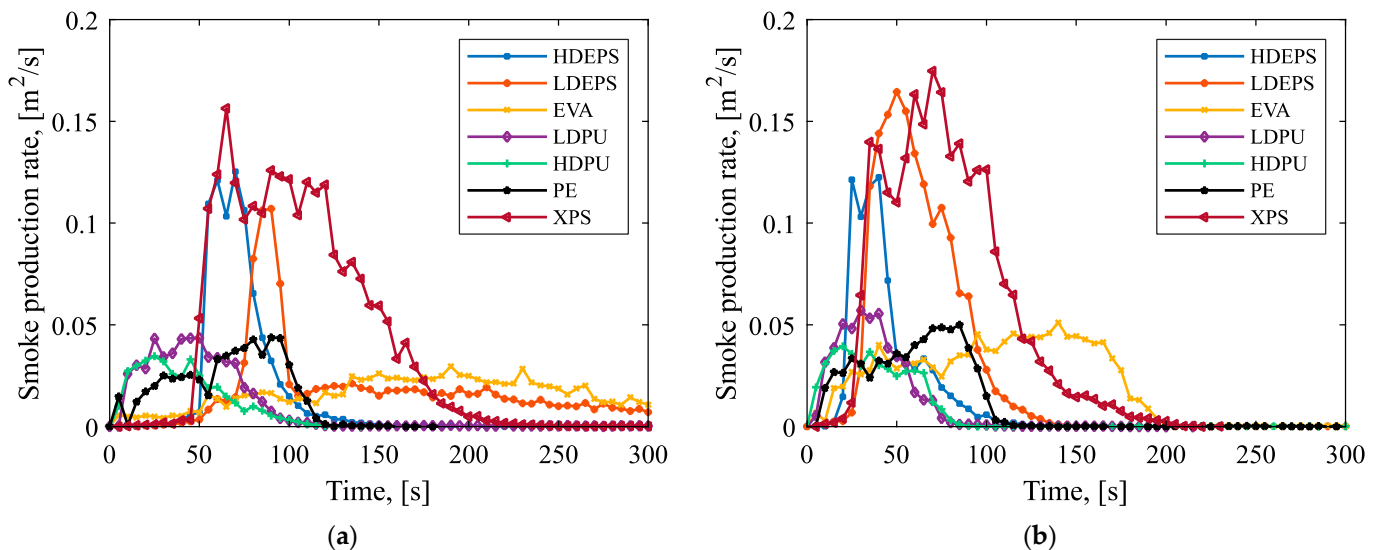


Figure 5. SPR time profile of polymer samples at (a) $35 \text{ kW}/\text{m}^2$; (b) $50 \text{ kW}/\text{m}^2$ heat fluxes.

3.2.1. Time to Ignition

CC test conditions typically represent a developing fire scenario attained after ignition in well-defined flaming conditions achieved by external cone radiation. TTI along with pHRR can be an indicator of flashover propensity [51]. It was observed that all the samples ignited under radiative heat fluxes of $35 \text{ kW}/\text{m}^2$ and $50 \text{ kW}/\text{m}^2$. The shortest TTI was recorded for HDPU, which ignited almost instantly upon exposure to radiative heat with a TTI of 3 s at $35 \text{ kW}/\text{m}^2$ and 2 s at $50 \text{ kW}/\text{m}^2$ heat fluxes, respectively. On the other hand, HDEPS took the longest to ignite with a TTI of 78 s at $35 \text{ kW}/\text{m}^2$ and 28 s at $50 \text{ kW}/\text{m}^2$ heat fluxes, respectively. HDEPS also took the longest time to flame out, extinguishing at 570 s at $35 \text{ kW}/\text{m}^2$ and 181 s at $50 \text{ kW}/\text{m}^2$ heat flux burnings (detailed in Table A1).

3.2.2. Mass Loss Profile and Residue

Mass loss measurements are important parameters in CC testing as HRR is dependent on mass loss rate, in which the degradation in the mass of the specimen led to spontaneous thermal reactions. It was observed that all the samples completely burned out, leaving very little residue (<20%) at the end of the test except for EVA, which retained a residual weight of approximately 20–27%. This finding corresponds to the TGA result where

EVA was found to retain the highest residual weight (22.7%) among all the test samples. Furthermore, LDPU had the highest peak mass loss rate (MLR) with a peak MLR of 23.53 g/s.m² at 50 kW/m² incident radiation (detailed in Table A1). Correlating MLR with pHRR corresponds to the finding that LDPU was also found to have the highest pHRR at 50 kW/m² incident radiation. The values of peak MLR and residual weight % for all the samples at the two heat fluxes are given in Table A1.

3.2.3. Peak Heat Release Rate

As expected, higher pHRR was observed for all the test samples at a higher heat flux of 50 kW/m² compared with pHRR at 35 kW/m² heat flux testing. The lowest peak was recorded for EVA with a pHRR of 258 kW/m² at 35 kW/m² heat flux and 393 kW/m² at 50 kW/m² heat flux, respectively. This agrees well with the TGA result, which established EVA as the most thermally stable polymer with highest degradation temperature amongst the test samples. Interestingly, XPS was recorded to have the highest pHRR of 633 kW/m² at 35 kW/m² incident radiation, while LDPU had the highest pHRR of 758 kW/m² at 50 kW/m² incident radiation. A possible explanation for this is that LDPU has two reaction peaks as observed from the TGA test result, therefore, in a CC test, the higher heat flux will cause the two reactions to occur closer together, resulting in a higher pHRR profile. Overall, this shows that exposure of polymers to higher heat fluxes can alter their thermal properties and can be extremely hazardous with a possibility of ignition within a few seconds with a high amount of heat release.

3.2.4. Total Heat Release

As expected, higher pHRR was observed for all the test samples at a higher heat flux. LDEPS was found to have the lowest THR of about 13 MJ/m². It is to be noted that, although EVA was recorded to have the lowest pHRR, it was found to have the highest THR (63~64 MJ/m²) among all the test samples as it sustained a much longer burning period with consistently high HRR. This demonstrates the importance of considering THR along with HRR for a more inclusive thermal fire hazard assessment of materials (detailed in Table A1).

3.2.5. Smoke Production

Smoke production parameters, such as smoke production rate (SPR) and total smoke release (TSR) deduced from the CC test, are crucial when considering visual obscuration due to smoke leading to compromised tenability during fire events. It was observed that the SPR curves correspond to the HRR curves with higher smoke produced at higher incident heat flux burning. XPS, HDEPS, and LDEPS were observed to have significantly higher SPR compared to the other samples. Furthermore, XPS was recorded to have the highest smoke release with TSR approximately 3 times higher than the average TSR of the other test samples. This agrees well with the fact that XPS is expected to produce high smoke densities releasing aromatic volatiles especially during incomplete gas-phase combustion [52].

3.3. Smoke Toxicity

3.3.1. FTIR Toxic Species Data

The presence of various toxic gas species in the smoke effluent produced during the CC testing of the polymer samples was confirmed by qualitative analysis of the FTIR spectra. A detailed analysis of the evaluating technique is demonstrated by considering the FTIR spectra of HDPU combusted at 50 kW/m² (at a specific time), as shown in Figure 6. Some of the major bands of interest are the peaks at 1500–1550 cm⁻¹ due to N-O stretching in the nitro compounds [53], 1647 cm⁻¹ due to C=C stretching in alkene [53], and 1733 cm⁻¹ due to C=O stretching in aliphatic aldehyde [54]. A strong peak at 2363 cm⁻¹ can be attributed to C≡N stretching in nitriles [55] and O=C=O stretching in CO₂ [56]. The peak at 1465 cm⁻¹ suggests -CH₂ deformation [57]. IR peaks at higher ranges, 3380 cm⁻¹ and 3649 cm⁻¹,

corresponding to N-H stretching [58], and O-H stretching [56], respectively. The functional groups identified in the IR spectra of HDPU can be attributed to the presence of various asphyxiants such as CO and HCN, and irritant gases including, HCHO, NO_x, ammonia, aldehydes, and acrolein in the HDPU smoke effluent [59]. The identified compounds corresponding to the peaks of the IR spectrum agree well with the toxic species reported in the FTIR test data that are used for the smoke toxicity assessment of the polymers.

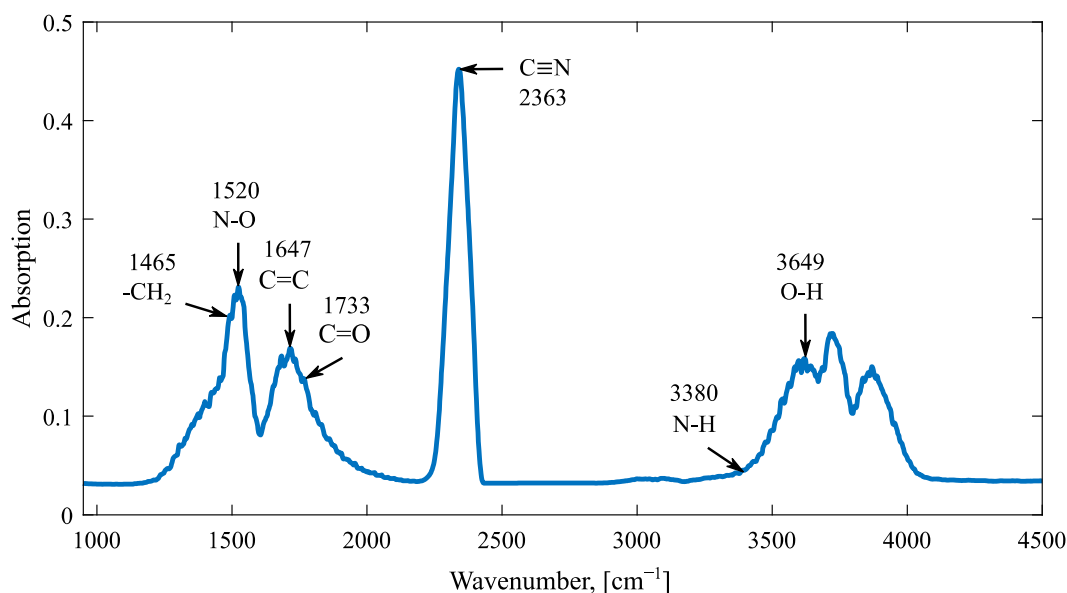


Figure 6. FTIR spectra of HDPU foam combusted at 50 kW/m².

Polymers, such as PE, EVA, and EPS, containing carbon and hydrogen mostly yield hydrocarbon species during combustion. Furthermore, oxidative degradation of these polymers produces CO, CO₂, and H₂O. PUs containing nitrogen in their elemental composition can produce HCN and oxides of nitrogen during combustion. Yields of some of the major gaseous species during the combustion of polymers contributing to their overall toxicity are shown in Figure 7a–d. The profile of the CO₂ concentration curves corresponds well to the profile of the HRR curves, resonating peak concentrations at the same timeline as peak HRRs. On the other hand, the CO concentration curves exhibited irregular trend lines with multiple peaks. It was observed that polystyrene polymers, HDEPS and XPS, yielded significantly more CO compared to the other polymers. Owing to the presence of nitrogen in its elemental composition, a significantly high concentration of HCN and NO was recorded for LDPU and HDPU, which is about 8.6 × HCN concentration and 91 × NO concentration compared with the polymers with the lowest concentration. This contributes significantly to the high overall toxicity of LDPU and HDPU. Interestingly, a significant concentration of NO was also found in PE and EVA during the stage of fully developed fire, which may be due to the presence of nitrogen in additives or cross-link agents.

3.3.2. Quantification of Toxic Hazards

Fire toxicity is commonly expressed in terms of fractional effective dose (FED) as discussed in Section 1. The basis of the methods used in the generation of toxic potency data assumes the additive nature of the individual concentration of toxicants present in the fire effluent [11]. ISO 13344 [19] presents two equations to estimate the lethality of fire effluent by FED calculation based on the N-gas model (FED_{N1}) and the Purser model (FED_{N2}) for a test time of 30 min. The LC₅₀ values, which is the lethal concentration of the fire effluent that is lethal to 50% of the exposed population, are taken from the same set of rat lethality data for both equations. A higher FED represents the higher toxicity of the test sample [32].

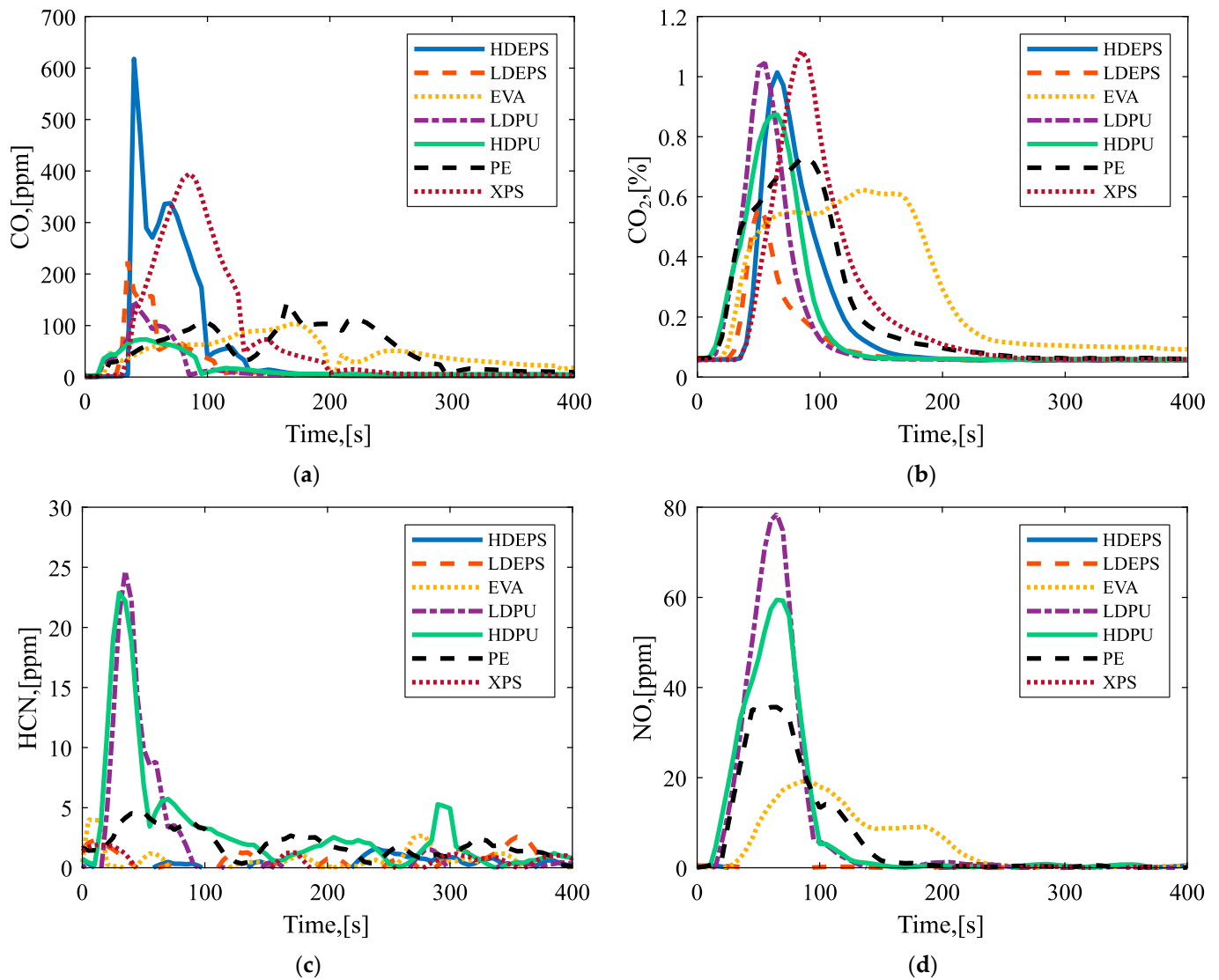


Figure 7. Concentrations of toxic gas emissions as a function of time at 50 kW/m² heat flux. (a) CO; (b) CO₂; (c) HCN; (d) NO.

N-gas equation [19]:

$$FED_{N1} = \frac{m[CO]}{[CO_2] - b} + \frac{21 - [O_2]}{21 - LC_{50,O_2}} + \frac{[HCN]}{LC_{50,HCN}} + \frac{[HCl]}{LC_{50,HCl}} + \frac{[HBr]}{LC_{50,HBr}} + \dots \quad (1)$$

$$\text{where } m = \begin{cases} -18 & [CO_2] < 5\% \\ 23 & [CO_2] > 5\% \end{cases}$$

$$b = \begin{cases} 122,000 & [CO_2] < 5\% \\ -38,600 & [CO_2] > 5\% \end{cases}$$

The values m and b are the slope and intercept, respectively, of the [CO]-vs- [CO₂] curve depicting the increasing toxicity of CO with the increase in CO₂ concentration.

Purser equation [19]:

$$FED_{N2} = \left\{ \frac{[CO]}{LC_{50,CO}} + \frac{[CN]}{LC_{50,HCN}} + \frac{[AGI]}{LC_{50,AGI}} + \frac{[OI]}{LC_{50,OI}} + \dots \right\} \times V_{CO_2} + A + \frac{21 - [O_2]}{21 - 5.4} \quad (2)$$

$$\text{where, } V_{\text{CO}_2} = 1 + \frac{\exp(0.14[\text{CO}_2]) - 1}{2}$$

$$A = [\text{CO}_2] \times 0.05$$

V_{CO_2} is a multiplication factor representing hyperventilation driven by CO_2 and A is an acidosis factor.

FED equations given in ISO 13344 [19] are often simplified to consider only three gases, O_2 , CO , and CO_2 , measured using a CC for quick toxicity assessment [31]. The rationale behind this is that smoke toxicity can be reasonably assessed by considering only these three major gas species. With this consideration, expressions FED_{N1} and FED_{N2} are simplified as FED_1 and FED_2 , respectively.

$$\text{FED}_1 = \frac{m[\text{CO}]}{[\text{CO}_2] - b} + \frac{21 - [\text{O}_2]}{21 - \text{LC}_{50,\text{O}_2}} \quad (3)$$

$$\text{FED}_2 = \frac{[\text{CO}]}{\text{LC}_{50,\text{CO}}} \times V_{\text{CO}_2} + A + \frac{21 - [\text{O}_2]}{21 - 5.4} \quad (4)$$

However, many studies have demonstrated that fire load can contain a wide range of toxic gas species such as NO_x , HCN , and HCl if halogens and N are present in their elemental composition or as additives and fire retardants [32,60]. Therefore, failing to consider these gas species can lead to an underestimation of the potential smoke toxicity of polymers. All four FED expressions, FED_{N1} , FED_{N2} , FED_1 , and FED_2 were considered in this study to compare the FED values and assess their reliability in evaluating the smoke toxicity of the polymer samples.

Figure 8a,b show the FED values of all the test samples calculated by using Equations (1)–(4) based on different assumptions, burned in well-ventilated conditions in the CC apparatus at 35 kW/m^2 and 50 kW/m^2 immediate heat fluxes. As expected, the FED values of the polymers increased at higher heat flux due to a higher level of fuel decomposition and thus, increasing the release of volatile species. The figures show higher values of FED_{N1} and FED_{N2} compared with FED_1 and FED_2 for all the test samples. This is obvious as equations FED_{N1} and FED_{N2} include all the major toxic gas species as identified and quantified by the CC-FTIR arrangement while equations FED_1 and FED_2 consider the concentration of only three gases, CO , O_2 , and CO_2 as recorded by the CC. The difference in the FED values is not quite substantial for various types of polystyrenes (LDEPS, HDEPS, and XPS) and polyethylene (PE and EVA) as they mainly consist of C and H in their elemental composition and the resulting major gaseous species produced (CO , O_2 , and CO_2) are included in the FED_1 and FED_2 equations. However, the difference is particularly significant for LDPU and HDPU which contains N as products of isocyanates in its elemental composition, resulting in the formation of HCN and highly reactive NO during the combustion process, which contributed to about 75–79% of the total FED_{N2} values. Furthermore, for both types of PUs (LDPU and HDPU), there was an increment of up to 223% in the FED_{N1} value compared with FED_1 and up to 400% increment in the FED_{N2} value compared with FED_2 at 50 kW/m^2 heat fluxes. This demonstrates a discrepancy in reporting the smoke toxicity of materials in some literature using only CC data compared to a more inclusive approach using the CC-FTIR. Overall, it was found that FED_{N2} , calculated using the Purser equation [19] (Equation (2)) considering all major toxic gas species, gave a higher FED value for all the polymer samples with up to 8 times FED compared to the FED_1 . Therefore, by taking a conservative approach to smoke toxicity assessment, FED_{N2} values are used in the fire performance assessment in the subsequent sections. By using this approach, the order of smoke toxicity (FED_{N2}) at 50 kW/m^2 heat flux is LDPU > HDPU > PE > HDEPS > XPS > EVA > LDEPS. Furthermore, LDPU, HDPU, and PE have FED_{N2} values higher than 0.3, which is typically the safety threshold suggested by fire engineers while considering smoke toxicity [61], suggesting that direct inhalation of effluents from these foams can be quite harmful to the exposed population. It should be noted that combustion in CC takes place in a well-ventilated condition and therefore underreports the possibility of smoke toxicity

of the fire effluent in a real large-scale under-ventilated fire. Nevertheless, this result can be used as an estimate for identifying the potentially toxic gas species present in the smoke effluent and to perform a comparative assessment of smoke toxicity of the polymers in a similar well-ventilated test condition.

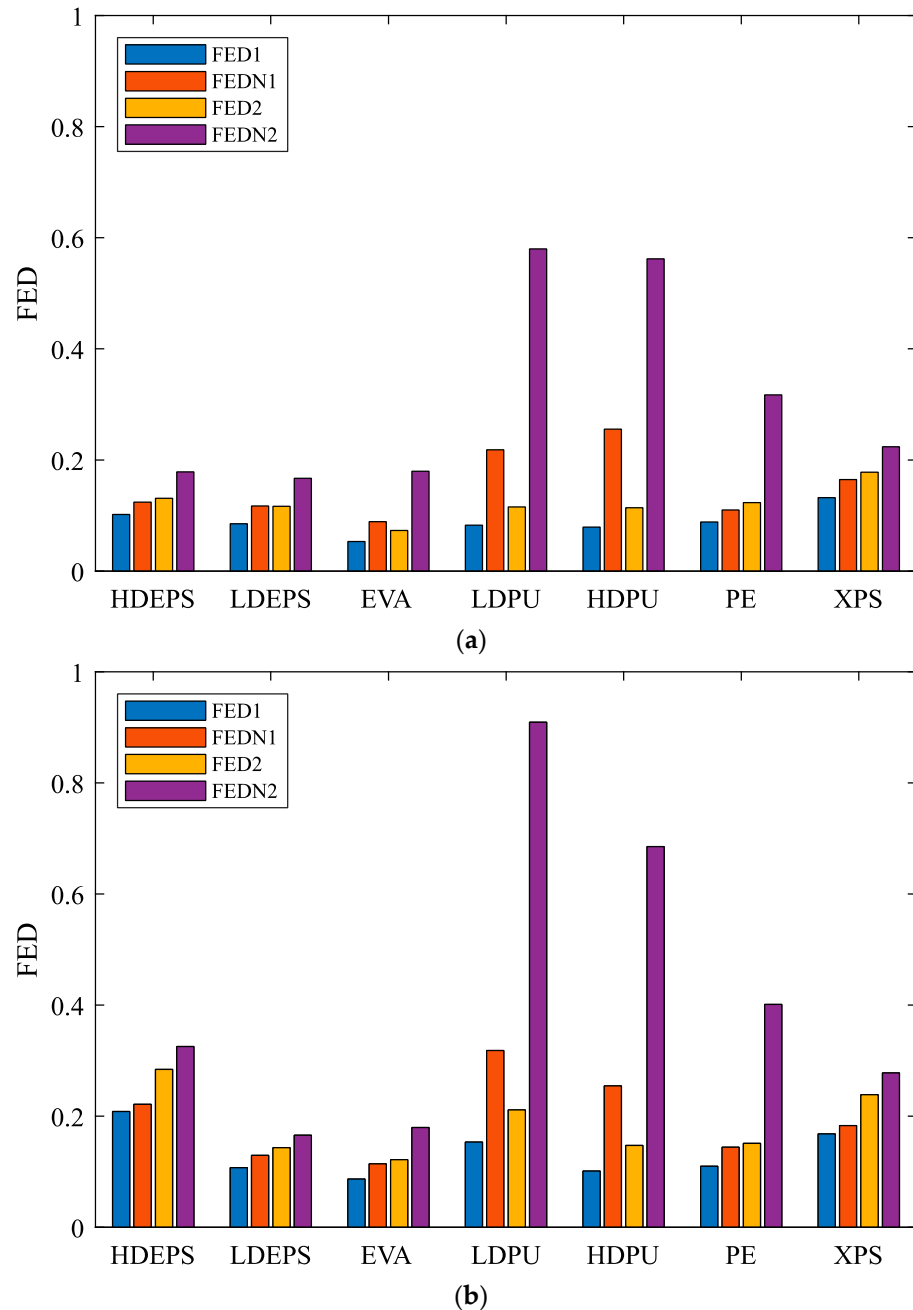


Figure 8. Fractional effective dose of polymers at (a) 35 kW/m² and (b) 50 kW/m² heat fluxes.

An alternative way of expressing the smoke toxicity of material, LC₅₀ [23] is:

$$LC_{50} = \frac{M}{FED \times V} \tag{5}$$

where M is the mass loss during the combustion process and V is the total air volume in the apparatus at standard pressure and temperature (V can be assumed as 0.01 m³ for bench scale testing) [31] (results summarized in Table A1).

3.4. Fire Hazard Assessment

This part of the paper aims to integrate the thermal hazard and potential smoke toxicity characteristics of the polymers to present a fire hazard profile of the polymers. The concept originally proposed by Petrella [51] used two risk parameters, flashover propensity (X) and total heat release (Y), to perform a full-scale fire hazard assessment of the test samples using cone calorimeter data. In this study, the original concept of Petrella [51] is extended by including another risk parameter, potential toxic hazard (Z), to account for the smoke toxicity aspect of the polymers as done by Chow et al. [40].

X (Flashover propensity/ $\text{kJ}/\text{m}^2\text{s}^2$)

$$X = \frac{\text{pHRR}}{\text{TTI}} \quad (6)$$

Y (Total heat release/ MJ/m^2)

$$Y = \text{THR} \quad (7)$$

Z (Toxic hazard/ m^3/g)

$$Z = \frac{1000}{\text{LC}_{50}} \quad (8)$$

Several studies have used the ratio of pHRR to TTI to signify the flashover propensity of materials. The rationale behind this is that a shorter duration of ignition time and higher pHRR are required for flashover to occur [51]. Flashover propensity can be combined with THR data obtained from the CC to better understand the full-scale fire behaviour of materials. Flashover propensity, which is based on pHRR, is mostly dependent on external parameters such as incident heat flux, ventilation condition, and degree of vitiation, while THR is fairly independent of these external environmental parameters and is a measure of the intrinsic chemical energy of the materials [51]. Furthermore, smoke hazard, Z, which is dependent on burning conditions as well as the chemical composition of the materials, is included in a holistic fire performance assessment of the polymers to present a more complete picture of fire hazard. This approach has been used in several literature works to assess the fire hazards of combustibles [40].

A 3-D risk diagram has been developed for the polymers comprising the three hazard parameters, flashover propensity (X), total heat released (Y), and toxic hazard (Z) at two radiative heat fluxes $35 \text{ kW}/\text{m}^2$ and $50 \text{ kW}/\text{m}^2$ as shown in Figure 9. At $50 \text{ kW}/\text{m}^2$ radiative heat flux, HDPU, was found to have the highest propensity for flashover with about 11.7 times flashover propensity (X) compared with the least flammable polymer (EPS), while EVA was found to have the highest THR with 5 times total heat release (Y) compared with the polymer with the lowest total heat release (LDEPS). Furthermore, LDPU was found to have the highest toxic hazard potential with about 6.7 times toxic hazard (Z) compared to the polymer with the least toxic hazard (EVA). It should be noted while the hazard diagram has the potential to present a comprehensive picture of the overall potential fire hazard considering the thermal characteristics and potential smoke toxicity of combustible materials, the toxic hazard presented in this paper is limited to a well-ventilated burning scenario in the CC.

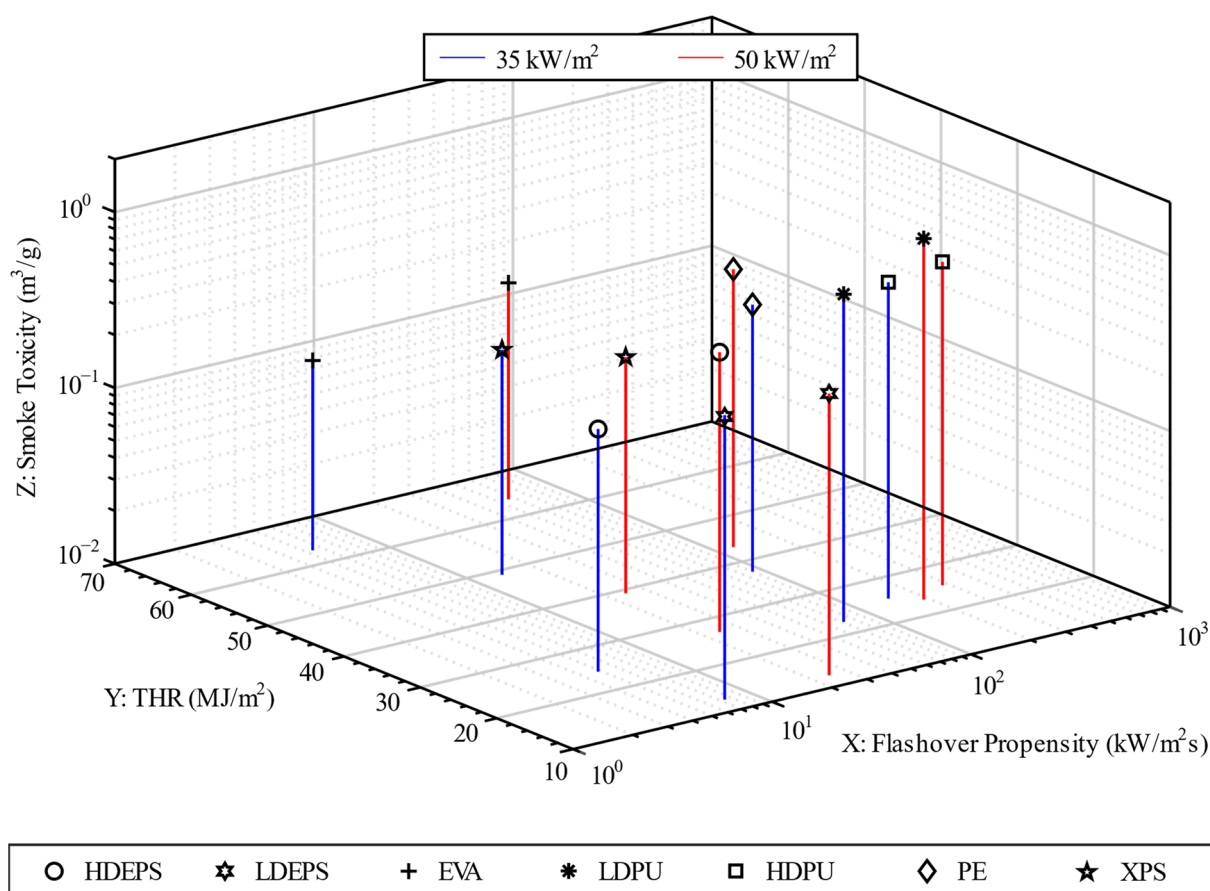


Figure 9. Risk diagram profile of polymer samples combusted at 35 kW/m² and 50 kW/m² heat fluxes.

4. Conclusions

In this article, a systematic method for fire hazard evaluation of polymeric materials was undertaken. Fire performance of various commonly available polymeric foams in the Australian market was evaluated by considering their thermal and smoke aspects using TGA, and a CC coupled with an FTIR instrument. TG and DTG curves were derived from the TGA testing in an inert nitrogen environment at 20 K/min to evaluate the thermal stability of the polymer samples. Various thermal and smoke properties, including pHRR, THR, TTI, ML, SPR, and TSR, as well as potential smoke toxicity, were analysed by using CC-FTIR test results at two radiative heat fluxes, 35 kW/m² and 50 kW/m². Four FED expressions were evaluated and compared to assess the potential smoke toxicity of the polymers using different assumptions. Furthermore, an overall fire hazard assessment of the polymers was carried out by considering three different hazard parameters, flashover propensity (X), total heat released (Y), and potential toxic hazard (Z).

Based on the TGA test results, it was observed that LDPU and HDPU had the least thermal stability with the lowest peak degradation temperatures. On the other hand, EVA exhibited the best thermal stability with the highest peak degradation temperature and retained the highest residual weight (22.7% wt) among all the test samples. According to the CC test, it was observed that all the polymeric samples ignited under both radiative heat fluxes. Upon exposure to 50 kW/m² heat flux, HDPU ignited almost instantly with a TTI of 2 s while some polymers including EPS and XPS took longer to ignite with a TTI of 28 s and 27 s, respectively. With the increment in incident heat flux from 35 kW/m² to 50 kW/m², a significant increase in pHRR was observed while THR remained relatively stable as this mostly depends on the inherent properties of the polymers rather than external burning conditions. XPS and LDPU were recorded to have the highest pHRR of 633 kW/m² for XPS at 35 kW/m² heat flux, and 758 kW/m² for LDPU at 50 kW/m² heat flux. On the other

hand, EVA was found to have the lowest pHRR of 258 kW/m^2 at 35 kW/m^2 heat flux, and 393 kW/m^2 at 50 kW/m^2 heat flux. Furthermore, EVA was found to have $5\times$ greater THR (64 MJ/m^2) compared with the one with the lowest THR of 13 MJ/m^2 (LDEPS). XPS was recorded to have the highest smoke release with $3\times$ greater TSR compared with the average TSR of the other test samples. Both TGA and CC testing found EVA to retain the maximum residual weight of about 20–27% of the total sample weight.

The smoke toxicity of the test samples was analysed by considering all the major toxic gases, including CO, CO₂, O₂, HCN, acid gases, and organic irritants, and was expressed in terms of FED. Four FED expressions were used to compare the potential smoke toxicity of the samples in a well-ventilated CC test condition using different assumptions. FED_{N2} calculated using Purser's equation [18] was found to give the most conservative estimation giving the maximum FED values for all the test samples. The difference in the FED calculated was particularly significant for both HDPU and LDPU where there was an increment of up to 79% in FED_{N2} compared to FED₂ because of the high concentration of HCN and NO in the fire effluent of HDPU and LDPU which FED₂ failed to include as it considers only the asphyxiant gases. Overall, at 50 kW/m^2 , HDPU exhibited 11.7 times flashover propensity (X) compared to the least flammable polymer (EPS), while EVA exhibited 5 times total heat release (Y) compared to the polymer with the lowest total heat release (LDEPS). Furthermore, LDPU exhibited 6.7 times potential toxic hazard (Z), compared to the polymer with the least toxic hazard potential (EVA). In conclusion, it was observed that engineering polymers have a high affinity for flashover, with the potential to release a significant amount of heat and toxic gases. Therefore, careful assessment of the overall fire performances of combustible polymers is essential before integrating them into buildings and furniture. Additionally, it will be worthwhile for the regulators to include smoke toxicity along with other fire parameters such as TTI and HRR to assess the fire performances of building materials capturing the whole range of potential fire hazards.

Author Contributions: Conceptualization, A.C.Y.Y.; Data curation, P.M.D. and L.L.; Formal analysis, P.M.D. and L.L.; Funding acquisition, G.H.Y.; Methodology, P.M.D. and T.B.Y.C.; Resources, C.W.; Software, T.B.Y.C.; Supervision, A.C.Y.Y., I.K. and G.H.Y.; Validation, L.L.; Visualization, C.W.; Writing—original draft, P.M.D.; Writing—review & editing, A.C.Y.Y. and I.K. All authors have read and agreed to the published version of the manuscript.

Funding: The paper is sponsored by the Australian Research Council (ARC Industrial Training Transformation Centre IC170100032). All financial and technical supports are greatly appreciated.

Institutional Review Board Statement: Not applicable.

Informed Consent Statement: Not applicable.

Data Availability Statement: Not applicable.

Acknowledgments: The authors hereby acknowledge the support by the fire testing laboratory for at the School of Mechanical and Manufacturing Engineering, UNSW Sydney, Australia.

Conflicts of Interest: The authors declare no conflict of interest. The funders had no role in the design of the study; in the collection, analyses, or interpretation of data; in the writing of the manuscript; or in the decision to publish the results.

Nomenclature

A	Acidosis factor
ACM	Aluminium composite material
CC	Cone calorimeter
CO	Carbon monoxide
CO ₂	Carbon dioxide
C ₃ H ₄ O	Acrolein
DTG	Derivative thermogravimetry
EIFS	Exterior insulation finish systems
EVA	Ethylene-vinyl acetate
FED	Fractional effective dose
FIDO	Fire Incident Data Organization
FTIR	Fourier transform infrared spectroscopy
FTT	Fire Testing Technology
GW	Glass wool
HRR	Heat release rate
HCN	Hydrogen cyanide
HCHO	formaldehyde
HDEPS	High-density expanded polystyrene
HDFU	High-density polyurethane
HCL	Hydrogen chloride
LC ₅₀	Lethal concentration
LDEPS	Low-density expanded polystyrene
LDPU	Low-density polyurethane
ML	Mass loss
N	Nitrogen
NFPA	National Fire Protection Association
NO	Nitrogen monoxide
NO ₂	Nitrogen dioxide
NO _x	Oxides of nitrogen
NH ₃	Ammonia
PE	Polyethylene
PhF	Phenolic foam
pHRR	peak heat release rate
PIR	Polyisocyanurate
PS	Polystyrene
PU	Polyurethane
SPR	Smoke production rate
SW	Stone wool
TG	Thermal degradation
TGA	Thermogravimetric analysis
THR	Total heat release
TSR	Total smoke released
TTI	Time to ignition
WRB	Weather-resistive barriers
XPS	Extruded polystyrene

Appendix A

Table A1. Experimental test results and calculations.

Polymers	HDEPS		LDEPS		EVA		LDPU		HDPU		PE		XPS	
Heat Flux (kW/m ²)	50	35	50	35	50	35	50	35	50	35	50	35	50	35
Peak [CO] (ppm)	617	291	224	177	103.35	49.28	148.07	85.33	73	66.82	145	90.33	394.85	248.58
Peak [CO ₂] (%)	1.01	0.39	0.56	0.51	0.62	0.36	1.04	0.6	0.87	0.65	0.72	0.63	1.08	0.73
Mass (g)	8.48	8.60	5.02	5.26	20.50	20.51	8.27	8.35	10.27	10.42	11.63	10.99	13.31	13.11
Residual wt (%)	7.78	16.27	16.93	18.63	20.29	26.76	2.53	4.19	3.44	14.77	10.23	12.82	6.76	13.72
Peak MLR (g/s.m ²)	20.18	12.10	14.24	12.99	9.75	6.65	23.53	14.69	17.42	15.21	12.30	10.70	20.38	14.14
Thickness (mm)	25	25	25	25	25	25	25	25	25	25	30	30	30	30
m	−18	−18	−18	−18	−18	−18	−18	−18	−18	−18	−18	−18	−18	−18
b	122,000	122,000	122,000	122,000	122,000	122,000	122,000	122,000	122,000	122,000	122,000	122,000	122,000	122,000
FED ₁	0.21	0.1	0.11	0.08	0.09	0.05	0.15	0.08	0.1	0.08	0.11	0.09	0.17	0.13
FED _{N1}	0.22	0.12	0.13	0.12	0.11	0.09	0.32	0.22	0.26	0.26	0.14	0.11	0.18	0.16
V _{CO2}	1.08	1.03	1.04	1.04	1.05	1.03	1.08	1.04	1.06	1.05	1.05	1.05	1.08	1.05
A	0.05	0.02	0.03	0.03	0.03	0.02	0.05	0.03	0.04	0.03	0.04	0.03	0.05	0.04
FED ₂	0.28	0.13	0.14	0.12	0.12	0.073	0.21	0.12	0.15	0.11	0.15	0.12	0.24	0.18
FED _{N2}	0.33	0.18	0.17	0.17	0.28	0.18	0.9	0.58	0.69	0.56	0.4	0.32	0.28	0.22
LC ₅₀ (g/m ³)	2527.85	4019.01	2472.48	2455.37	5689.83	8317.94	878.57	1367.45	1441.59	1583.76	2590.6	3008.1	4460.74	5032.01
TSR	900.6	673	445.8	457	708.2	593.5	283.8	306.3	241.2	216.9	376.2	328.9	1419.2	1356.7
TTI (s)	28	78	18	48	7	48	4	6	2	3	4	5	27	46
pHRR (kW/m ²)	670.94	377.95	439.47	362.1	393.04	258.45	758.63	425.49	563.79	447.75	488.63	451.11	655.44	632.36
THR (MJ/m ²)	26.76	24.57	12.68	13.01	64.05	63.15	23.45	22.8	25.48	25.37	43.4	37.46	39.21	48.97
X (kW/m ² .s)	23.96	4.85	24.42	7.54	56.15	5.38	189.66	70.92	281.9	149.25	122.16	90.22	24.28	13.75
Y (MJ/m ²)	26.76	24.57	12.63	13.01	64.05	63.15	23.45	22.8	25.48	25.37	43.4	37.46	39.21	48.97
Z (m ³ /g)	0.39	0.24	0.4	0.4	0.17	0.12	1.13	0.73	0.69	0.63	0.38	0.33	0.22	0.19

References

1. Peng, L.; Ni, Z.; Huang, X. Review on the fire safety of exterior wall claddings in high-rise buildings in China. *Procedia Eng.* **2013**, *62*, 663–670. [\[CrossRef\]](#)
2. Jia, D.; Yang, J.; He, J.; Li, X.; Yang, R. Melamine-based polyol containing phosphonate and alkynyl groups and its application in rigid polyurethane foam. *J. Mater. Sci.* **2021**, *56*, 870–885. [\[CrossRef\]](#)
3. Badrock, G. Post incident analysis report: Lacrosse Docklands, 25 November 2014. *MATEC Web Conf.* **2016**, *46*, 6002. [\[CrossRef\]](#)
4. McKenna, S.T.; Jones, N.; Peck, G.; Dickens, K.; Pawelec, W.; Oradei, S.; Harris, S.; Stec, A.A.; Hull, T.R. Fire behaviour of modern façade materials—Understanding the Grenfell Tower fire. *J. Hazard. Mater.* **2019**, *368*, 115–123. [\[CrossRef\]](#) [\[PubMed\]](#)
5. White, N. *Fire Hazards of Exterior Wall Assemblies Containing Combustible Components*; Springer: Berlin/Heidelberg, Germany, 2015. [\[CrossRef\]](#)
6. Yuen, A.C.Y.; Chen, T.B.Y.; Li, A.; De Cachinho Cordeiro, I.M.; Liu, L.; Liu, H.; Lo, A.L.P.; Chan, Q.N.; Yeoh, G.H. Evaluating the fire risk associated with cladding panels: An overview of fire incidents, policies, and future perspective in fire standards. *Fire Mater.* **2021**, *45*, 663–689. [\[CrossRef\]](#)
7. Hossain, M.D.; Hassan, M.K.; Akl, M.; Pathirana, S.; Rahnamayiezekavat, P.; Douglas, G.; Bhat, T.; Saha, S. Fire Behaviour of Insulation Panels Commonly Used in High-Rise Buildings. *Fire* **2022**, *5*, 81. [\[CrossRef\]](#)
8. Chen, T.B.Y.; Yuen, A.C.Y.; Yeoh, G.H.; Yang, W.; Chan, Q.N. Fire Risk Assessment of Combustible Exterior Cladding Using a Collective Numerical Database. *Fire* **2019**, *2*, 11. [\[CrossRef\]](#)
9. Clarke, F.B. Fire Death Scenario and Firesafety Planning. *Fire J.* **1976**, *70*, 2022.
10. Putorti, J.A.; McElroy, J. interFIRE, A site dedicated to improving fire investigation worldwide. *Tech. Rep.* **1998**, 4009.
11. Stec, A.; Hull, R. *Fire Toxicity*; Woodhead Publishing: Cambridge, UK, 2010. [\[CrossRef\]](#)
12. Yuen, A.C.Y.; Chen, T.B.Y.; Wang, C.; Wei, W.; Kabir, I.; Vargas, J.B.; Chan, Q.N.; Kook, S.; Yeoh, G.H. Utilising genetic algorithm to optimise pyrolysis kinetics for fire modelling and characterisation of chitosan/graphene oxide polyurethane composites. *Compos. Part B Eng.* **2020**, *182*, 107619. [\[CrossRef\]](#)
13. Yuen, A.C.Y.; Chen, T.B.Y.; De Cachinho Cordero, I.M.; Liu, H.; Li, A.; Yang, W.; Cheung, S.C.P.; Chan, Q.N.; Kook, S.; Yeoh, G.H. Developing a solid decomposition kinetics extraction framework for detailed chemistry pyrolysis and combustion modelling of building polymer composites. *J. Anal. Appl. Pyrolysis* **2022**, *163*, 105500. [\[CrossRef\]](#)
14. Hartzell, G.E. Engineering analysis of hazards to life safety in fires: The fire effluent toxicity component. *Safety Sci.* **2001**, *38*, 147–155. [\[CrossRef\]](#)
15. *Europe Is Playing with Fire: A Call to Action on Fire Safety in Buildings*; European Parliament: Brussels, Belgium, 2014.
16. Babrauskas, V. Fire Safety Improvements in the combustion toxicity area: Is there a role for LC50 tests? *Fire Mater.* **2000**, *24*, 113–119. [\[CrossRef\]](#)
17. Yuen, A.C.Y.; Yeoh, G.H.; Yuen, R.K.K.; Chen, T. Numerical simulation of a ceiling jet fire in a large compartment. *Procedia Eng.* **2013**, *52*, 3–12. [\[CrossRef\]](#)
18. Purser, D.A. Toxicity assessment of combustion products. In *SFPE Handbook of Fire Protection Engineering*; SFPE: Gaithersburg, MD, USA, 2002.
19. International Organization for Standardization. (ISO) 13344; Estimation of the Lethal Toxic Potency of Fire Effluents. ISO: Geneva, Switzerland, 2015.
20. Yuen, A.C.Y.; Chen, T.B.Y.; Yang, W.; Wang, C.; Li, A.; Yeoh, G.H.; Chan, Q.N.; Chan, M.C. Natural ventilated smoke control simulation case study using different settings of smoke vents and curtains in a large atrium. *Fire* **2019**, *2*, 7. [\[CrossRef\]](#)
21. IEC. IEC 60695-7-1:2010; Fire Hazard Testing—Part 7-1: Toxicity of Fire Effluent—General Guidance. IEC: Geneva, Switzerland, 2010; p. 50.
22. International Organization for Standardization. (ISO) 13344; Determination of the Lethal Toxic Potency of Fire Effluents. ISO: Geneva, Switzerland, 1996.
23. International Organization for Standardization. (ISO) 13571; Life-Threatening Components of Fire—Guidelines for the Estimation of Time to Compromised Tenability in Fires. ISO: Geneva, Switzerland, 2012.
24. International Organization for Standardization. (ISO/TR) 9122-4; Toxicity Testing of Fire Effluents—Part 4: The Fire Model (Furnaces and Combustion Apparatus Used in Small-Scale Testing). ISO: Geneva, Switzerland, 1993.
25. ASTM E 1678-02; Standard Test Method for Measuring Smoke Toxicity for Use in Fire Hazard Analysis. ASTM International: West Conshohocken, PA, USA, 2002.
26. NFPA 269; Standard Test Method for Developing Toxic Potency Data for Use in Fire Hazard Modeling. NFPA: Quincy, MA, USA, 2000.
27. Han, S.S.; Chow, W.K. Calculating FED and LC50 for testing toxicity of materials in bench-scale tests with a cone calorimeter. *Polym. Test.* **2005**, *24*, 920–924. [\[CrossRef\]](#)
28. Fateh, T.; Richard, F.; Batiot, B.; Rogaume, T.; Luche, J.; Zaida, J. Characterization of the burning behavior and gaseous emissions of pine needles in a cone calorimeter—FTIR apparatus. *Fire Saf. J.* **2016**, *82*, 91–100. [\[CrossRef\]](#)
29. Sharma, A.; Mishra, K.B. Experimental investigations on the influence of ‘chimney-effect’ on fire response of rainscreen façades in high-rise buildings. *J. Build. Eng.* **2021**, *44*, 103257. [\[CrossRef\]](#)
30. Singh, H.; Jain, A.K. Ignition, Combustion, Toxicity, and Fire Retardancy of Polyurethane Foams: A Comprehensive Review. *J. Appl. Polym. Sci.* **2008**, *111*, 1115–1143. [\[CrossRef\]](#)

31. Chow, C.L.; Han, S.S.; Han, G.Y.; Hou, G.L.; Chow, W.K. Assessing smoke toxicity of burning combustibles by four expressions for fractional effective dose. *Fire Mater.* **2020**, *44*, 804–813. [CrossRef]
32. Stec, A.A.; Hull, T.R. Assessment of the fire toxicity of building insulation materials. *Energy Build.* **2011**, *43*, 498–506. [CrossRef]
33. Peck, G.; Jones, N.; McKenna, S.T.; Glockling, J.L.D.; Harbottle, J.; Stec, A.A.; Hull, T.R. Smoke toxicity of rainscreen façades. *J. Hazard. Mater.* **2021**, *403*, 123694. [CrossRef]
34. Jones, N.; Peck, G.; McKenna, S.T.; Glockling, J.L.D.; Harbottle, J.; Stec, A.A.; Hull, T.R. Burning behaviour of rainscreen façades. *J. Hazard. Mater.* **2021**, *403*, 123894. [CrossRef] [PubMed]
35. Guillaume, E.; Fateh, T.; Schillinger, R.; Chiva, R.; Ukleja, S. Study of fire behaviour of facade mock-ups equipped with aluminium composite material-based claddings, using intermediate-scale test method. *Fire Mater.* **2018**, *42*, 561–577. [CrossRef]
36. Yuen, A.C.Y.; Yeoh, G.H.; Alexander, B.; Cook, M. Fire scene investigation of an arson fire incident using computational fluid dynamics based fire simulation. *Build. Simul.* **2014**, *7*, 477–487. [CrossRef]
37. Yuen, A.C.Y.; Yeoh, G.H.; Alexander, R.; Cook, M. Fire scene reconstruction of a furnished compartment room in a house fire. *Case Stud. Fire Saf.* **2014**, *1*, 29–35. [CrossRef]
38. Choi, J.H.; Chae, S.U.; Hwang, E.H.; Choi, D.M. Fire Propagation Characteristics and Fire Risks of Polyurethanes: Effects of Material Type (Foam & Board) and Added Flame Retardant. *Fire* **2022**, *5*, 105.
39. Liu, L.; Chen, T.B.Y.; Yuen, A.C.Y.; Doley, P.M.; Wang, C.; Lin, B.; Liang, J.; Yeoh, G.H. A systematic approach to formulate numerical kinetics for furnishing materials fire simulation with validation procedure using cone/FT-IR data. *Heat Mass Transf.* **2021**, *1*, 1–19. [CrossRef]
40. Chow, W.K.; Han, S.S.; Zeng, W.R. Assessment of fire performance of typical furniture foams with and without fire retardants using a cone calorimeter. *Cell. Polym.* **2010**, *29*, 73–94. [CrossRef]
41. Quintiere, J.G. Scaling applications in fire research. *Fire Saf. J.* **1989**, *15*, 3–29. [CrossRef]
42. Open Cell Foam Perth–Foam Sales. Perth, Australia. Available online: <https://www.foamsales.com.au/collections/open-cell-foam> (accessed on 11 June 2022).
43. TG 209 F1 Libra®-NETZSCH Analyzing & Testing. Selb, Germany. Available online: <https://analyzing-testing.netzsch.com/en-AU/products/thermogravimetric-analysis-tga-thermogravimetry-tg/tg-209-f1-libra> (accessed on 15 May 2022).
44. The i series of Cone Calorimeters. East Grinstead, UK. Available online: <https://www.fire-testing.com/iconic-mini-and-iconic-classic-calorimeters/> (accessed on 22 May 2022).
45. *International Organization for Standardization (ISO) 5660-1; Reaction-to-Fire Tests—Heat Release, Smoke Production and Mass Loss Rate—Part 1: Heat Release Rate (Cone Calorimeter Method) and Smoke Production Rate (Dynamic Measurement)*. ISO: Geneva, Switzerland, 2015.
46. Babrauskas, V.; Harris, R.H.; Braun, E.; Levin, B.C.; Paabo, M.; Gann, R.G. *The Role of Bench-Scale Test Data in Assessing Real-Scale Fire Toxicity*; Technical Note 1284; National Bureau of Standards and Technology: Washington, DC, USA, 1991.
47. Hull, T.R.; Schartel, B. Development of fire-retardant materials-Interpretation of cone calorimeter data. *Fire Mater.* **2007**, *31*, 327–354.
48. atmosFIR-Analyser Product Range. Protea Ltd., Middlewich, UK. Available online: <https://www.protea.ltd.uk/atmosfir> (accessed on 17 June 2022).
49. Al-Sayegh, W.A.; Aljumaiah, O.; Andrews, G.E.; Phylaktou, H.N. PVC Cable Fire Toxicity Using the Cone Calorimeter. In *Fire Science and Technology 2015*; Springer: Singapore, 2017; pp. 175–182. [CrossRef]
50. *International Organization for Standardization. (ISO) 19702; 2015 Guidance for Sampling and Analysis of Toxic Gases and Vapours in Fire Effluents Using Fourier Transform Infrared (FTIR) Spectroscopy*. ISO: Geneva, Switzerland, 2015.
51. Petrella, R.V. The Assessment of Full-Scale Fire Hazards from Cone Calorimeter Data. *J. Fire Sci.* **1994**, *12*, 14–43. [CrossRef]
52. Woolley, W.D.; Raftery, M.M. Smoke and toxicity hazards of plastics in fires. *J. Hazard. Mater.* **1975**, *1*, 215–222. [CrossRef]
53. Trivedi, M.K.; Patil, S.; Shettigar, H.; Bairwa, K.; Trivedi, M.K.; Patil, S.; Shettigar, H.; Bairwa, K.; Spec, S.J.; Acta, A. Spectroscopic Characterization of Chloramphenicol and Tetracycline: An Impact of Biofield Treatment. *Pharm. Anal. Acta* **2015**, *6*, 395. [CrossRef]
54. Clare, T.L.; Swartz, N.A. Characterization of High Performance Protective Coatings for Use on Culturally Significant Works. In *Intelligent Coatings for Corrosion Control*; Butterworth-Heinemann: Oxford, UK, 2015; pp. 641–671. [CrossRef]
55. Rajakumar, G.; Gomathi, T.; Thiruvengadam, M.; Devi Rajeswari, V.; Kalpana, V.N.; Chung, I.M. Evaluation of anti-cholinesterase, antibacterial and cytotoxic activities of green synthesized silver nanoparticles using from *Millettia pinnata* flower extract. *Microb. Pathog.* **2017**, *103*, 123–128. [CrossRef]
56. Ngohang, F.E.; Fontaine, G.; Gay, L.; Bourbigot, S. Smoke composition using MLC/FTIR/ELPI: Application to flame retarded ethylene vinyl acetate. *Polym. Degrad. Stab.* **2015**, *115*, 89–109. [CrossRef]
57. Yan, L.; Xu, Z.; Wang, X. Progress in Organic Coatings Synergistic effects of organically modified montmorillonite on the flame-retardant and smoke suppression properties of transparent intumescent fire-retardant coatings. *Prog. Org. Coat.* **2018**, *122*, 107–118. [CrossRef]
58. Rus, A.Z.M. Biopolymers for superhydrophobic photocatalytic coatings. In *Biopolymers and Biotech Admixtures for Eco-Efficient Construction Materials*; Woodhead Publishing: Cambridge, UK, 2016; pp. 421–447. [CrossRef]
59. Landry, T.D.; Daems, D.; Pauluhn, J.; Reimann, K.A. *Polyurethane Products in Fires: Acute Toxicity of Smoke and Fire Gases*; International Isocyanate Institute: New York, NY, USA, 2002.

-
60. Alarifi, A.; Andrews, G.E.; Witty, L.; Phylaktou, H.N. Ignition and toxicity of selected aircraft interior materials using the cone calorimeter and FTIR analysis. In *Conference Proceedings, Interflam2013*; Interscience Communications Ltd.: London, UK, 2013; Volume 1, pp. 37–49.
 61. Molyneux, S.; Stec, A.A.; Hull, T.R. The effect of gas phase flame retardants on fire effluent toxicity. *Polym. Degrad. Stab.* **2014**, *106*, 36–46. [[CrossRef](#)]